Biochimica et Biophysica Acta, 977 (1989) 227–232
Elsevier

BBABIO 40230

BBA Report

ENDOR studies of the intermediate electron acceptor radical anion $I^{\cdot -}$ in Photosystem II reaction centers

W. Lubitz [1,*], R.A. Isaacson [2], M.Y. Okamura [2], E.C. Abresch [2], M. Plato [3] and G. Feher [2]

[1] *Institut für Organische Chemie, Freie Universität, Berlin (Germany),* [2] *University of California at San Diego, La Jolla, CA (U.S.A.) and* [3] *Institut für Molekülphysik, Freie Universität, Berlin (Germany)*

(Received 10 July 1989)

Key words: Photosystem II; Cytochrome *b*-559 D_1D_2 complex; Intermediate electron acceptor; Pheophytin; ENDOR

The EPR and ENDOR characteristics of the intermediate electron acceptor radical anion $I^{\cdot -}$ in Photosystem II (PS II) are shown to be identical in membrane particles and in the D_1D_2 cytochrome *b*-559 complex (Nanba, O. and Satoh, K. (1987) Proc. Natl. Acad. Sci. USA 84, 109–112). These findings provide further evidence that the D_1D_2 complex is the reaction center of PS II and show that the pheophytin binding site is intact. A hydrogen bond between $I^{\cdot -}$ and the protein (GLU D1-130) is postulated on the basis of D_2O exchange experiments. The ENDOR data of $I^{\cdot -}$ and of the pheophytin *a* radical anion in different organic solvents are compared and the observed differences are related to structural changes of the molecule on the basis of molecular orbital calculations (RHF-INDO/SP). The importance of the orientation of the vinyl group (attached to ring I) on electron transfer is discussed.

Recently a Photosystem (PS) II complex containing only the D_1, D_2 and cytochrome *b*-559 subunits was isolated by Satoh et al. [1]. Its pigment composition is similar to that of bacterial reaction centers (RC's) [2] (4–5 chlorophylls, 2 pheophytins, 1 non-heme Fe^{2+}), but it is devoid of quinone. The D_1 and D_2 subunits show a remarkable sequence homology to the L and M subunits of the bacterial RCs [3,4], adding support that D_1D_2 is the RC of PS II.

The D_1D_2 complex performs the primary charge separation forming the radical pair state $P^+I^{\cdot -}$, where P is the primary donor (P-680) and I the intermediate acceptor [5]. Time-resolved optical spectroscopy showed the charge-transfer complex to form in a few picoseconds with lifetimes in the nanosecond range [6–8].

For a basic understanding of the structure–function relationship in photosynthetic systems, a knowledge of the electronic structure of the reactants is required. Two useful methods to explore the electronic distribution of the radical species are EPR and ENDOR (electron-nuclear double resonance) spectroscopy [9]. By these techniques the electron-nuclear hyperfine couplings (hfc's) can be determined. The hfc's are related to the electron spin density at the respective nuclei. Thus, a map of the valence electron spin distribution over the molecule is obtained; it provides a sensitive measure of structural changes of the radical and its surrounding.

In this paper we focus on the intermediate electron acceptor radical anion $I^{\cdot -}$. In previous work by Fajer and coworkers on PS II membrane particles, EPR and ENDOR were used along with other techniques to identify this species with the radical anion of Pheo *a* (see Fig. 1) and to measure some of the hfc's [10–12]. Improved ENDOR spectrometer sensitivity and resolution has enabled us to measure additional hfc's with higher accuracy. This made a detailed comparison between $I^{\cdot -}$ in PS II membrane particles and in the D_1D_2 complex possible.

Recently we reported on the ENDOR detection of the hfc that arises from the proton of GLU L104 hydrogen bond to $I^{\cdot -}$ in bacterial RCs [13]. The existence of a similar H bond between $I^{\cdot -}$ and GLU D1-130 in the D_1D_2 complex [4] is supported by recent FTIR data [14]. Here we present ENDOR data that

Abbreviations: ENDOR, electron-nuclear double resonance; RHF-INDO/SP, restricted Hartree-Fock-intermediate neglect of differential overlap spin polarization; PS II, Photosystem II; Chl, chlorophyll; Pheo, pheophytin; MTHF, 2-methyltetrahydrofuran; RC, reaction center; MO, molecular orbital; FTIR, Fourier transform infrared; SCF, self-consistent field; hfc, hyperfine coupling.

* Present address: Zweites Physikalisches Institut, Universität Stuttgart, Stuttgart, F.R.G.

Correspondence: G. Feher, University of California at San Diego, Department of Physics, B-019, La Jolla, CA 92093, U.S.A.

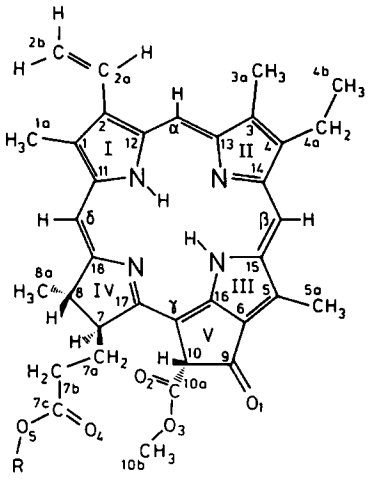

Fig. 1. Molecular structure and numbering scheme of pheophytin *a* (Pheo *a*).

provide further evidence for such a linkage. A preliminary report of this work has been given [15].

Pheophytin *a* was obtained by treatment of Chl *a* (Sigma) with HCL (0.01 M) in methanol. Photosystem-II-enriched subchloroplast fragments (called membrane particles) were prepared from spinach as described [16]. The D_1D_2 cytochrome *b*-559 complex was isolated and purified as described by Nanba and Satoh [1]. The Triton (0.05%) was exchanged by digitonin (0.2%) during the final purification step on the DEAE (Toyopearl) column; this increased the thermal stability of the complex. The optical spectrum was identical to that described [1,17]. As a functional assay the pheophytin photoreduction was measured yielding $\Delta A_{450}/A_{675} \approx 0.06$ [1,17].

The intermediate electron acceptor radical anion I^- was generated in the PS II membrane particles ($A_{680} = 400$, 0.1 M Tricine buffer, 0.05% Triton X-100, 50% glycerol) by illumination with white light (500 W projection lamp) for 60 s at 0 °C (ice/water) in the presence of 50 mM sodium dithionite, followed by rapid freezing in liquid nitrogen [12]. In the D_1D_2 preparation ($A_{675} = 30$, 50 mM Tris, 0.05% Triton X-100 or 0.2% digitonin) I^- was photoaccumulated in the presence of sodium dithionite (20 mM) and methyl viologen (50 μM) using the same illumination and freeze-trapping procedure. The D_2O exchange of the PS II membrane particles was performed by diluting the sample with D_2O buffer and reconcentrating it in centricon filters (repeated twice), followed by incubation at 23 °C for 20 h.

The radical anions of the model compound Pheo *a* (concn., 10^{-3} M) were prepared by: (i) electrolytic reduction in 2-methyltetrahydrofuran (MTHF) using tetra-*n*-butyl ammonium perchlorate as supporting electrolyte under high vacuum conditions (18); or (ii) illuminating the sample (in pyridine/10% water, 0.01 M Na_2S [19]) in an ice bath with strong white light (500 W projector) for approx. 2 min followed by rapid freezing in liquid nitrogen.

The 9 GHz EPR/ENDOR spectrometer used was described earlier [20]. A silvered quartz loop-gap resonator [21] replaced the microwave cavity to obtain sufficient sensitivity with small samples (approx. 30 μl).

Molecular orbital (MO) calculations of the electron spin distribution in the anion radicals were performed by an all-valence-electron self-consistent field (SCF) method. This method is based on the INDO parametrization and uses a restricted Hartree-Fock (RHF) approach with subsequent perturbation treatment of spin polarization effects (RHF-INDO/SP) (for details see Ref. 22). Calculations of the anisotropic hyperfine tensors were done for each nucleus using the full valence orbital spin density distribution of the molecule as described in Ref. 23.

The EPR characteristics of I^- in PS II and of Pheo a^- are in agreement with those reported earlier [10,11]. In Fig. 2 ^{1}H-ENDOR spectra of I^- and Pheo a^- in frozen solution ($T = 100$ K) are compared. The spectra of I^- in membrane particles (Fig. 2a) and in the D_1D_2 complex (Fig. 2b) are similar, differing only slightly in the widths of the resonance peaks. In contrast to the I^- radical in the protein matrix the Pheo a^- in an organic glass (Fig. 2c) exhibits broader lines. Apparently, the protein environment provides a better ordered and well-defined surrounding than a frozen solvent. In the latter the radical may be trapped in several conformational substates with slightly different structures and electron spin distributions leading to line broadening of the spectra. Similar observations have been made previously for other radicals in frozen solvents and protein matrices, e.g., for semiquinones [24] (see also Chap. 9 in Ref. 9).

In the spectra of Fig. 2 seven line pairs (labeled 1,1′ to 7,7′) centered around the proton Larmor frequency ν_H can be distinguished. The proton hfc's A_H, are obtained from the spacings of the line pairs according to the ENDOR resonance condition

$$\nu^{+}_{ENDOR} = |\nu_H \pm \tfrac{1}{2}A_H|$$

Two types of proton can be distinguished in these spectra: (i) those chemically bound to the radical itself, and (ii) those belonging to the surrounding solvent or protein molecules. The latter are only weakly coupled, giving rise to small, dipolar hfcs. Their ENDOR transitions occur close to the proton Larmor frequency ν_H in the so-called Matrix region (see Fig. 3). The chemically bound protons are more strongly coupled and exhibt large anisotropic hfc's. These resonances are usually difficult to detect in powder spectra with no orientational selection [9], since they are smeared out over the whole range of anisotropic hyperfine values. Exceptions are ENDOR resonances from methyl protons that are

still freely rotating at 100 K and exhibit an axially symmetric hf tensor [9]. Their hf anisotropy, defined as $|A_{\parallel} - A_{\perp}|/|A_{iso}|$ does not exceed 30%. Accordingly, the resonances 1,1′/2,2′ and 4,4′/5,5′ are assigned to the hyperfine tensor components $A_{\parallel}$ and $A_{\perp}$ of the methyl groups at positions 5a and 1a (see Fig. 1), respectively (see Fig. 3 in Ref. 24 for method of analysis). This assignment is based on selective deuteration of the 5a-methyl group in a similar radical [12]. The hyperfine tensor components of the methyl groups are given in Table I together with their isotropic values. Further

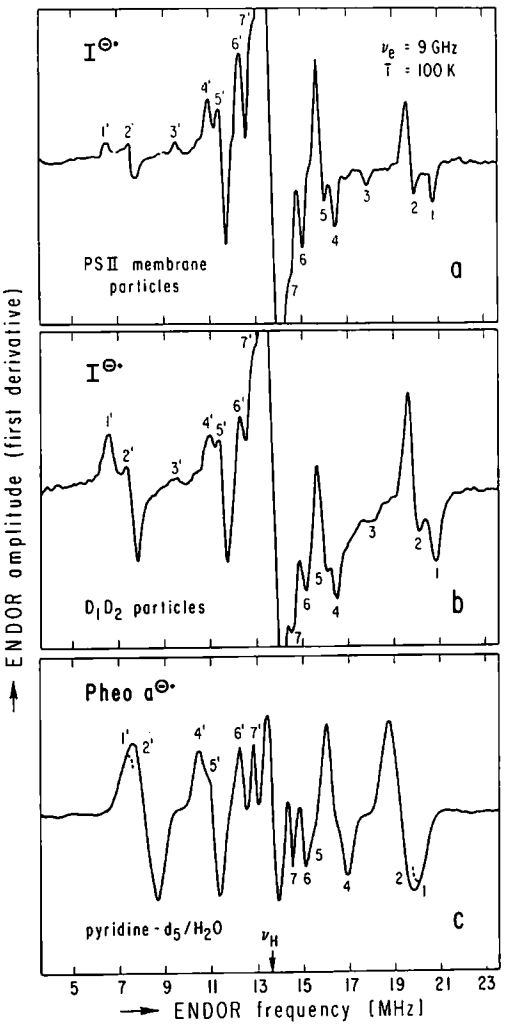

Fig. 2. ^{1}H-ENDOR spectra (frozen solution) of (a) $I^{\bar{\cdot}}$ in PS II membrane particles, detergent: Triton X-100, (b) $I^{\bar{\cdot}}$ in the D_1D_2 cytochrome *b*-559 complex, detergent: digitonin; the spectrum of $I^{\bar{\cdot}}$ in D_1D_2 in Triton X-100 is essentially the same, (c) Pheo $a^{\bar{\cdot}}$ in pyridine-d_5/water (10%); ν_H denotes the proton Larmor frequency, corresponding high- and low-frequency lines are numbered (1,1′ to 7,7′, see also Table I, 1 to 7); experimental conditions; $\nu_e = 9$ GHz; r.f. power, 20 W to produce a field of 4.5 Gauss (rotating frame), microwave power, 0.5 mW; 15 kHz frequency modulation ± 150 kHz deviation; temperature, 100 K; signal averaging time, 4 h. Relative line intensities (compare a and b) in ENDOR spectra depend strongly on the relaxation characteristics and on experimental conditions and are, therefore, not useful for comparison purposes. The central region of a has been expanded and is shown in Fig. 3.

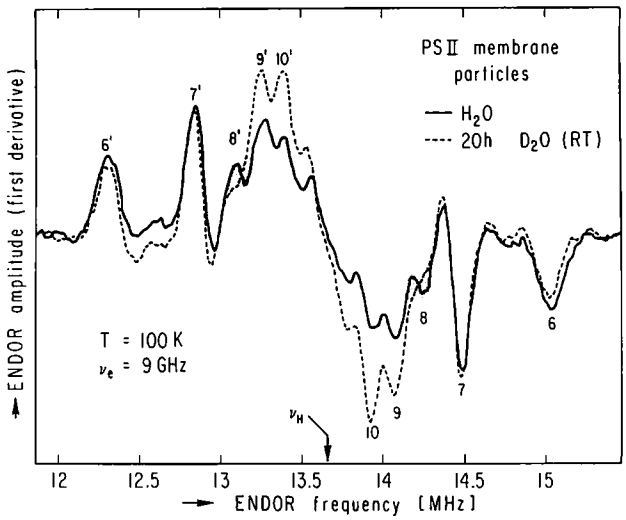

Fig. 3. ^{1}H-ENDOR spectrum (matrix region) of $I^{\bar{\cdot}}$ in PS II membrane particles incubated at room temperature in H_2O (solid line) and for 20 h in D_2O (dashed line); the shaded circles indicate a line pair belonging to an exchangeable proton; line pairs are numbered, for hfc's see Table I; experimental conditions: r.f. power 10 W to produce a field of 3 gauss (rotating frame); microwave power, 0.5 mW; 15 kHz frequency modulation ± 50 kHz deviation; $T = 100$ K, signal averaging time, 5 h.

assignments of the measured hfc's rely on theoretical calculations of the spin densities and the hyperfine tensors (see below).

Comparison of the hf data obtained for $I^{\bar{\cdot}}$ in PS II membrane particles (Fig. 2a) and in the D_1D_2 complex (Fig. 2b) shows that they are identical within experimental error. Although the spectrum of Pheo $a^{\bar{\cdot}}$ (Fig. 2c) is qualitatively similar to $I^{\bar{\cdot}}$, the hfc's differ significantly, (cf. Table I), in particular those of the two methyl groups in positions 1a and 5a that are attached to opposite sides of the molecule (see Fig. 1). $I^{\bar{\cdot}}$ in the RC protein exhibits an increased spin density at 5a by 13% and 23% and a decreased one at 1a by 13% and 18% as compared with Pheo $a^{\bar{\cdot}}$ in pyridine/water and MTHF, respectively. To explore changes of the electronic structure of Pheo $a^{\bar{\cdot}}$ caused by interactions with the environment, we measured the hfc's in the polar pyridine/water solvents and in the apolar ether MTHF (see Table I). In pyridine/water the spin density at 5a is increased by 9% and at 1a is decreased by 5% with respect to the apolar ether MTHF.

The matrix ENDOR region of $I^{\bar{\cdot}}$ in PS II membrane particles is shown in Fig. 3; the hfc's are given in Table I. Incubation of the system in D_2O (20 h) leads to the disappearance of a line pair (shaded circles) corresponding to a hfc of 1.1 MHz *. Exchangeable protons of the

* Such a line pair is absent in Pheo $a^{\bar{\cdot}}$ in pyridine/H_2O, and D_2O exchange shows only small effects on the matrix region. In this system a possible disordered H-bond leading to considerable line broadening may be present (see, e.g., Ref. 13).

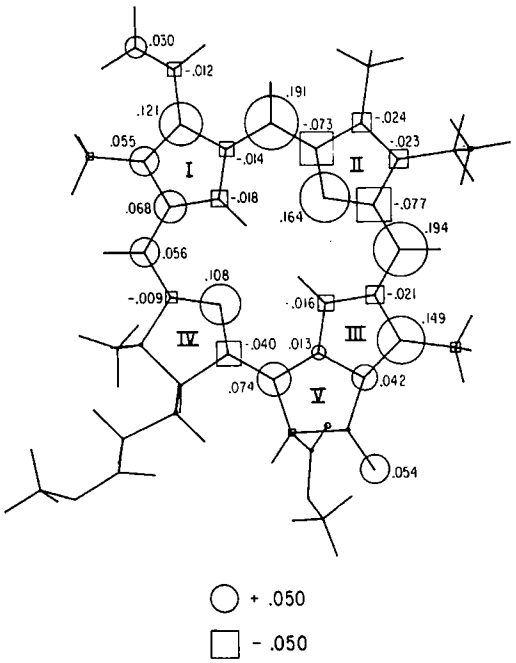

Fig. 4. Π spin densities (ρ^{π}) of Pheo $a^{\bar{\cdot}}$ calculated by RHF-INDO/SP, the values (see numbers) are proportional to the area of the circles ($\rho > 0$) or squares ($\rho < 0$). Mostly standard geometries were used except for rings I and V, which were obtained by minimization of the total energy. The vinyl group was rotated out of plane by 14° [27]. Approx. 98% of the unpaired electron spin is in the π (p_z) orbital, the rest in the p_x, p_y and s orbitals. The pronounced asymmetry of the spin-density distribution around the molecular axis running through N_I and N_{III} is due to the presence of the unsaturated ring II in Pheo $a^{\bar{\cdot}}$ (see Fig. 1) that couples ring II much stronger to the π system than ring IV. In bacterio-Pheo $a^{\bar{\cdot}}$, which has rings II and IV saturated, this asymmetry is much less pronounced.

Pheo a are those bound to the nitrogens and to C-10 (Fig. 1). However, these protons are expected to have large non-axial hyperfine tensors resulting in a spread of resonances over several MHz (see below) or the protons may exchange slowly (e.g., at C-10) and are, therefore, not expected to give rise to pronounced changes in the matrix region. Based on these considerations and on our recent results obtained for $I^{\bar{\cdot}}$ in bacterial RCs [13], the 1.1 MHz hfc is assigned to the $A_{\perp}$ component of the hyperfine tensor of a hydrogen that is bonded between $I^{\bar{\cdot}}$ (keto group of ring V) and the amino acid residue GLU D1-130 [4] *.

To interpret the ENDOR spectra and to relate the experimentally observed effects to structural alterations of the system we have performed MO calculations of the RHF-INDO/SP-type [22]. The isotropic hfc's arising from the s-orbitals, obtained from this calculation

* We cannot exclude that some water molecules are present in the RC and that one is hydrogen bonded to this keto group in $I^{\bar{\cdot}}$. However, this possibility seems unlikely in view of the recent EPR/ENDOR [13], FTIR [29] and X-ray structure [4,25] data of bacterial RC's.

TABLE I

Hyperfine coupling constants [MHz] for $I^{\bar{\cdot}}$ in PS II RC's and for Pheo $a^{\bar{\cdot}}$

All data from deconvolution of frozen-solution ^{1}ENDOR spectra ($T = 100$ K), error ± 0.1 MHz (except for overlapping lines marked with an asterisk *: ± 0.2 MHz).

Line number [a]	Tentative assignment [b]	Hyperfine component [c]	$I^{\bar{\cdot}}$ PS II [d]	Pheo a^{-} [e]	
				MTHF	d-pyridine/ H_2O
1	methyl 5a	$A_{\parallel}$	14.3	11.6 *	12.2 *
2		$A_{\perp}$	12.1	9.9	10.9
		A_{iso}	12.8	10.4	11.3
3	methine	A_i	8.0		
4	methyl 1a	$A_{\parallel}$	5.6	6.7	6.5
5		$A_{\perp}$	4.2	5.2	4.9
		A_{iso}	4.7	5.7	5.4
6	?	A_i	2.6	2.6	2.6
7	methyl 3a	$A_{\parallel,\perp}$	1.5	1.5	1.5
8	H-bond	$A_{\perp}$	1.1	–	–
9	?	A_i	0.7		
10	?	A_i	0.4		0.4

[a] For numbering of lines, see Figs. 2 and 3.

[b] Assignments of methyl groups 5a and 1a are based on their typical ENDOR characteristics [9,24] and specific deuteration [12]; all other rely on calculations of tensor components (see text), hfc's A_6, A_9 and A_{10} could arise from β proton (at positions 7, 8, 10) or even from vinyl (2a, 2b), or NH protons.

[c] Specific hyperfine tensor components are assigned to each value (e.g., $A_{\parallel}$ or $A_{\perp}$ for the methyl protons) and the isotropic hfc is calculated: $A_{iso} = \frac{1}{3}(2A_{\perp} + A_{\parallel})$, A_i denotes a non-specified component.

[d] Hyperfine values are identical for $I^{\bar{\cdot}}$ in PS II membrane particles and in the D_1D_2 cytochrome b-559 subcomplex (either in Triton X-100 or digitonin). Fajer et al. [11,12] reported average values of 12.5 (12.2) and 4.6 MHz for the methyl groups in 5a and 1a, respectively, for PS II membrane particles (130 K).

[e] For Pheo $a^{\bar{\cdot}}$ the matrix ENDOR region is less well resolved. Additional hfc's obtained from high resolution spectra are: 3.3 and 17.2 MHz. Fujita et al. [10] obtained average values of 10.5 and 5.5 MHz for the methyl protons in position 5a and 1a, respectively (at 133 K in dimethylformamide), Lendzian et al. [18] measured the isotropic values by liquid-state ENDOR/TRIPLE: +9.9 (5a methyl) and +5.4 MHz (1a methyl) in 1,2-dimethoxyethan at 263 K.

(not shown) are in good agreement with the data from liquid solution ENDOR (Ref. 18; see also Plato, M., unpublished results).

The anisotropic hfc's arise from the spin density in the p-orbitals. Most (approx. 98%) of the spin density resides in the π (p_z) orbital shown for Pheo $a^{\bar{\cdot}}$ in Fig. 4. Large positive values are calculated for the nitrogens in rings II and IV, for the methine positions (α, β, γ, δ), for various carbon positions in rings I and III and for the keto oxygen on ring V. The p_x and p_y orbitals contribute only a small amount (less than 2%) to the anisotropic hfc's, which were obtained from the spin-density distribution in all valence orbitals of the entire molecule (Plato, M., unpublished results). The strongly anisotropic non-axial hfc's for the methine, vinyl and

N-H protons make it difficult to detect these transitions by ENDOR. In contrast, the anisotropy of the methyl resonances is smaller and the tensors are almost axially symmetric. The experimentally determined anisotropy is larger for the methyl group at position 1a than for 5a by a factor of 1.7 (for I^-) and 2.0 (for Pheo a^-), although $A_{1a} < A_{5a}$. The calculated value is 1.62 in good agreement with experiment. The origin of the difference in anisotropies lies in the larger next nearest neighbor spin densities in the surrounding of the methyl group at 1a as compared with those near position 5a (see Fig. 4).

The hydrogen bond distance, r, between GLU D1-130 and O_1 (keto group on ring V) of I^- can be estimated from the simple point dipole relation [13]

$$A_H(\text{MHz}) = \frac{79}{r^3}\rho(3\cos^2\theta - 1)$$

where θ is the angle between the applied magnetic field and the line joining the two nuclei (H and O), ρ is the spin density at the contact position (9 keto oxygen), and r is the distance in Å between H and O. Assuming that the measured value of 1.1 MHz corresponds to the perpendicular component $|A_\perp|$ and $\rho^\pi_{O_1} = 0.054$ (Fig. 4) one obtains a hydrogen bond distance of $r_{OH} = 1.57$ Å *. This value is consistent with a fairly strong H-bond between GLU and the pigment and is in agreement with the FTIR data [14]. According to the MO calculation on Pheo a^- (using H_2O as an in-plane H-bond donor) such a bond would increase A_{5a} by approx. 5% and decrease A_{1a} by approx. 3%. These effects are small but are in the direction of the experimentally observed changes.

In bacterial RCs (*Rb. capsulatus*) GLU L104 (which forms a hydrogen bond to the 9-keto group of bacteriopheophytin) was changed to LEU, GLN and LYS [26]. The electron-transfer characteristics of the RCs from these mutants were only slightly affected (less than 50%). Thus, this residue is not the dominant contributor to the rate and directionality of the electron transfer in bacterial RCs. This is in agreement with our calculations which show only a small effect of this hydrogen bond on the electronic distribution of either bacterio-Pheo a^- on Pheo a^-. These findings are surprising in view of the fact that this residue is highly conserved in several bacterial species and in the D_1 of PS II [3,4].

The experimentally observed ratio of the isotropic methyl hfc's at 5a and 1a varies between 1.8 and 2.7 in different matrices (Table I). MO calculations show that this ratio depends stronly on the rotational angle θ of the vinyl group. For $\theta = 14°$ (see Plato, M., unpublished results) $\rho^\pi_{5a}/\rho^\pi_{1a}$ is 2.7 and the ratio of the calculated isotropic hfc's is 2.2. Rotating this substituent out of plane ($\theta = 90°$) decreases A_{1a} by 20% and increases A_{5a} by 11%. The direction and magnitude of these effects are in approximate agreement with the changes of the observed methyl hfc's (Table I) between Pheo a^- in organic solvents and I^- in the protein matrix; they are in agreement with the work of Forman et al. [12]. Comparing Pheo a^- in apolar (MTHF) and polar (pyridine/H_2O) solvents (Table I) shows that A_{1a} decreases by 5% and A_{5a} increases by 9%. A more polar solvent cage apparently polarizes the electron distribution of Pheo a^- causing the increase in A_{5a} and the (smaller) decrease in A_{1a}. This is in agreement with the existence of a polar keto group attached to ring III whereas ring I carries the apolar vinyl group. Additionally, a hydrogen bond between the keto group and a water molecule (in pyridine/H_2O) could increase this asymmetry (see above).

These observations lead to the hypothesis that a change of the Pheo a structure in the RC is due to a rotation of the vinyl group *. Pheo a in various organic solvents, does not seem to undergo such a rotation.

Based on the analogy to the bacterial RC [25] it can be assumed that the vinyl group is in the contact region between the Pheo and the preceding electron carrier, or a bridging molecule (e.g., Chl) in the D_1D_2 protein. It is therefore interesting to speculate that a change of the rotational angle of this group could optimize the orbital overlap and thereby the electron-transfer rate. Furthermore, this group might change its position in the charge-separated state thereby providing a 'conformational switch' that could inhibit wasteful back reactions.

This work was supported by the Deutsche Forschungsgemeinschaft (Sfb 312), by NATO (RG 86/0029), by the National Science Foundation (DMB 85-18922 and DMB 87-04920) and the National Institute of Health (GM 13191).

References

1 Nanba, O. and Satoh, K. (1987) Proc. Natl. Acad. Sci. USA 84, 109–112.
2 Okamura, M.Y., Feher, G. and Nelson, N. (1982) in Photosynthesis: Energy Conversion by Plants and Bacteria, Vol. 1 (Govindjee, ed.), Academic Press, New York, Ch. 5, pp. 195–272.

* An error in the theoretical spin density by a factor of 2 would change the distance by only 20–25%). Note that the H-bond geometry is determined for I^-; for the unreduced I state the hydrogen bonding could be different (e.g., weaker as postulated in Ref. 29).

* We have not discussed here the possibility of a structural change (e.g., puckering of the ring) of the pheophytin that may occur in the RC protein [28]. Such effects are difficult to assess experimentally or theoretically.

3 Komiya, H., Yeates, T.O., Rees, D.C., Allen, J.P. and Feher, G. (1988) Proc. Natl. Acad. Sci. USA 85, 9012–9016.
4 Michel, H. and Deisenhofer, J. (1988) Biochemistry 27, 1–7.
5 Okamura, M.Y., Satoh, K., Isaacson, R.A. and Feher, G. (1987) in Progress in Photosynthesis Research (Biggins, J., ed.), Vol. I, pp. 375–381, Martinus Nijhoff, Dordrecht.
6 Wasielewski, M.R., Johnson, D.G., Seibert, M. and Govindjee (1989) Proc. Natl. Acad. Sci. USA 86, 524–528.
7 Danielius, R.V., Satoh, K., Van Kan, P.J.M., Plijter, J.J., Nuijs, A.M. and Van Gorkum, H.J. (1987) FEBS Lett. 213, 241–244.
8 Takahashi, Y., Hanson, O., Mathis, P. and Satoh, K. (1987) Biochim. Biophys. Acta 893, 49–59.
9 Kurreck, H., Kirste, B. and Lubitz, W. (1988) Electron Nuclear Double Resonance Spectroscopy of Radicals in Solution, VCH Publishers, Weinheim.
10 Fujita, I., Davis, M.S. and Fajer, J. (1978) J. Am. Chem. Soc. 100, 6280–6282.
11 Fajer, J., Davis, M.S., Forman, A., Klimov, V.V., Dolan, E. and Ke, B. (1980) J. Am. Chem. Soc. 102, 7143–7145.
12 Forman, A., Davis, M.S., Fujita, I., Hanson, L.K., Smith, K.M. and Fajer, J. (1981) Isr. J. Chem. 21, 265–269.
13 Feher, G., Isaacson, R.A., Okamura, M.Y. and Lubitz, W. (1988) in The Photosynthetic Bacterial Reaction Center: Structure and Dynamics (Breton, J. and Verméglio, A., eds.), pp. 229–235, Plenum Press, New York.
14 Barillot, E., Nabedryk, E., Adrianambinintsoa, S., Mäntele, W. and Breton, J. (1989) Biophys. J. 55, 180a.
15 Lubitz, W., Plato, M., Feher, G., Isaacson, R.A. and Okamura, M.Y. (1988) Biophys. J. 53, 67a.
16 Kuwabara, T. and Murata, N. (1982) Plant Cell Physiol. 23, 533–539.
17 Barber, J., Chapman, D.J. and Telfer, A. (1987) FEBS Lett. 220, 67–73.
18 Lendzian, F., Möbius, K. and Lubitz, W. (1982) Chem. Phys. Lett. 90, 375–381.
19 Fajer, J., Forman, A., Davis, M.S., Spaulding, L.D., Brune, D.C. and Felton, R.H. (1977) J. Am. Chem. Soc. 99, 4134–4140.
20 Lubitz, W., Isaacson, R.A., Abresch, E.C. and Feher, G. (1984) Proc. Natl. Acad. Sci. USA 81, 7792–7796.
21 Hyde, J.S. and Froncisz, W. (1986) in Electron Spin Resonance, A Specialist Periodical Report, Vol. 10A, pp. 175–182, Alden Press, Oxford.
22 Plato, M., Tränkle, E., Lubitz, W., Lendzian, F. and Möbius, K. (1986) Chem. Phys. 107, 185–196.
23 Beveridge, D.L. and McIver, Jr., J.W. (1971) J. Chem. Phys. 54, 4681–4690.
24 Feher, G., Isaacson, R.A., Okamura, M.Y. and Lubitz, W. (1985) in Antennas and Reaction Centers of Photosynthetic Bacteria – Structure, Interactions and Dynamics (Michel-Beyerle, M.E., ed.), Vol. 42, pp. 174–189, Springer Series in Chemical Physics, Berlin.
25 Yeates, T.O., Komiya, H., Chirino, A., Rees, D.C., Allen, J.P. and Feher, G. (1988) Proc. Natl. Acad. Sci. USA 85, 7993–7997.
26 Bylina, E.J., Kirmaier, C., McDowell, L., Holten, D. and Youvan, D.C. (1988) Nature 336, 182–184.
27 Fischer, M.S., Templeton, D.H., Zalkin, A. and Calvin, M. (1972) J. Am. Chem. Soc. 94, 3613–3619.
28 Barkigia, K.M., Chantranupong, L., Smith, K.M. and Fajer, J. (1988) J. Am. Chem. Soc. 110, 7566–7567.
29 Mäntele, W.G., Wollenweber, A.M., Nabedryk, E. and Breton, J. (1988) Proc. Natl. Acad. Sci. USA 85, 8468–8472.